Time Reversal and Applications to imaging

Hongkai Zhao

Department of Mathematics
University of California, Irvine

Supported by ONR and DARPA.

Collaborators: M. Hou, K.Solna

Outline

- Introduction to time reversal.
  - The physical experiment.
  - Basic properties: auto-focusing and resolution.

- Application to array imaging.
  - Imaging point targets.
  - Imaging the shape of extended target.

Experimental setup.

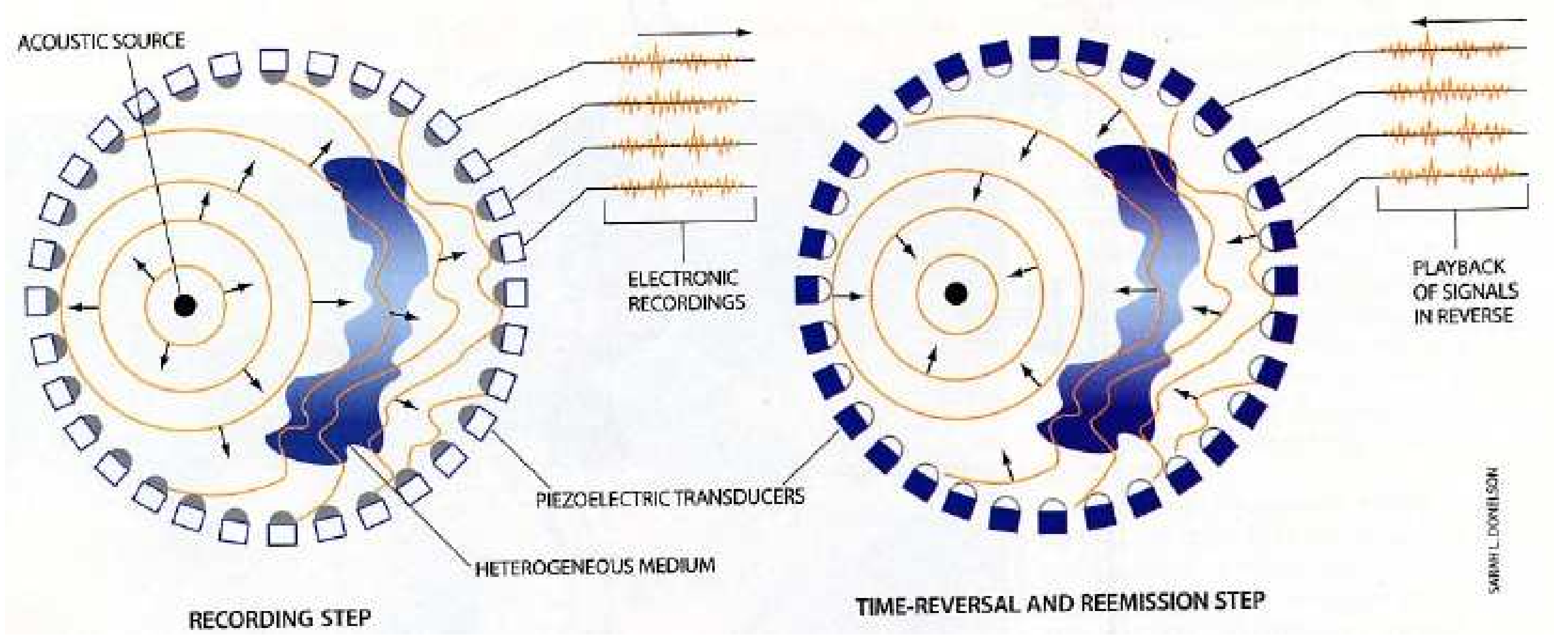

From Scientific American, November 1999, M. Fink.

Refocusing property of time reversal and its applications.

The time reversed and back propagated wavefield (through the same medium) refocuses on the source (or an illuminated scatter) due to *time reversibility and spatial reciprocity of waves*.

Applications:

- Active time reversal: time reversal is physically carried out in the real medium.
  - Automatic target detection and destruction.
  - Secure Communications.
- Passive time reversal: time reversal is carried out on computers through an "approximate" medium.
  - Nondestructive testing.
  - Identification and imaging of targets.

Medical applications.

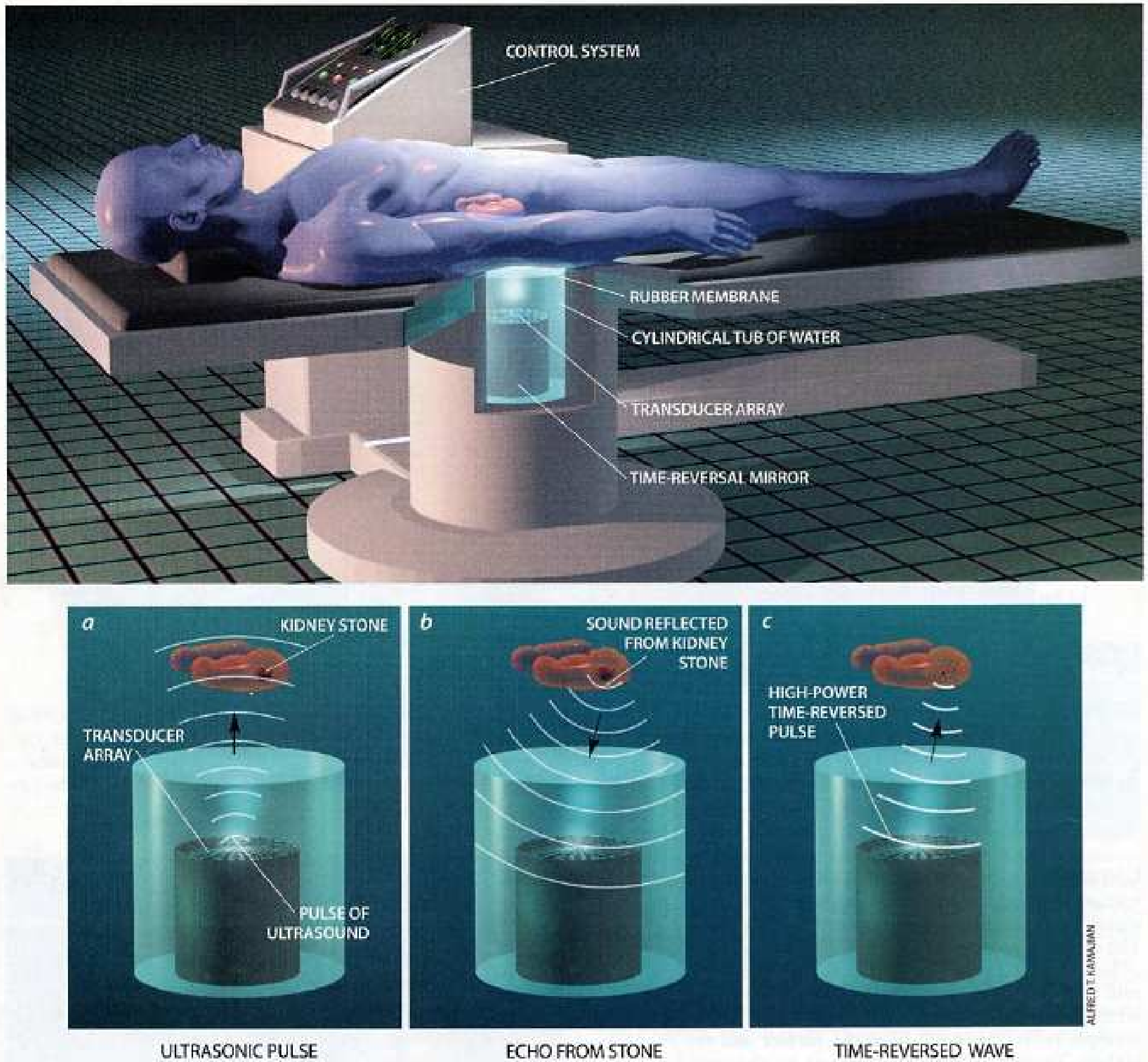

KIDNEY STONES can be targeted and broken up with ultrasound by using the self-focusing property of a time-reversal mirror. An ultrasonic pulse emitted by one part of the array (*a*) produces a distorted echo from the stone (*b*). A powerful time-reverse of this echo passes through intervening tissues and organs, focuses back on the stone (*c*) and breaks it up. Iterating the procedure improves the focus and allows real-time tracking as the stone moves because of the patient's breathing.

From Scientific American, November 1999, M. Fink.

Deterministic diffraction limit.

In homogeneous media:

- No resolution finer than the wave length λ.
- For small aperture time reversal mirror (TRM) the resolution is $\propto \frac{a}{L\lambda}$.

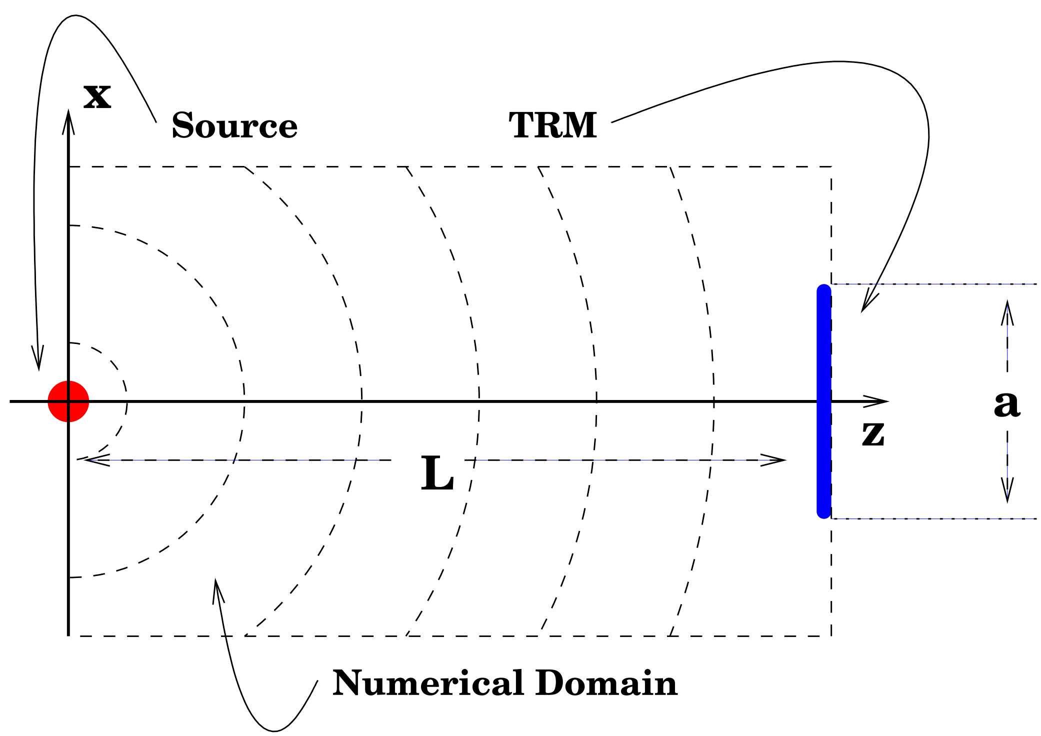

Time reversal in random media.

In random medium, (Blomgren, Papanicolaou & Zhao, JASA, 2001.)

- The inhomogeneities cause *multipathing* which can make the effective aperture a_e of the TRM larger and super-resolution occurs.

$$a_e \sim a\sqrt{1+\frac{2\gamma L^3}{a^2}}, \qquad \left\{ \begin{array}{ll} a & \text{Physical TRM aperture} \\ a_e & \text{Effective aperture} \\ L & \text{Propagation distance} \\ \gamma & \text{Medium constant.} \end{array} \right.$$

- The super-resolution is stable in time domain due to self-averaging of different frequencies.

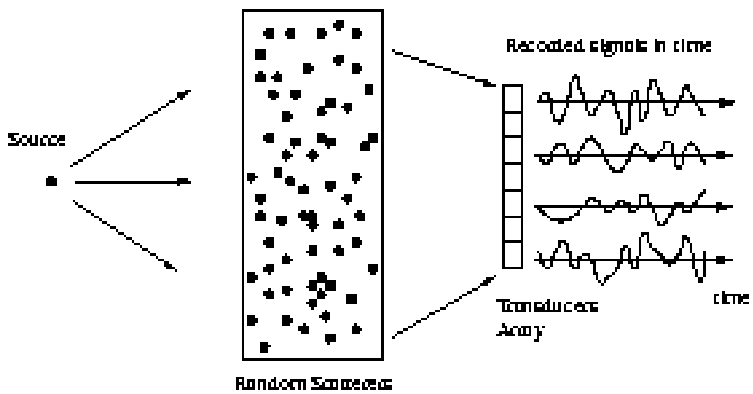

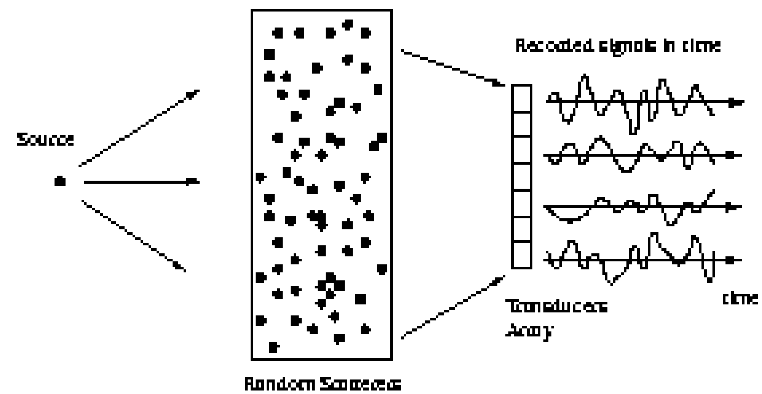

Remarks:

- Underwater sound (Kuperman et. al.) and ultrasound regime (Fink et. al.) experiments observe both *super-resolution* and *stability* of time reversal.
- Early work of Dowling-Jackson uses ensemble average to show super-resolution.

Time reversal vs. inverse filter

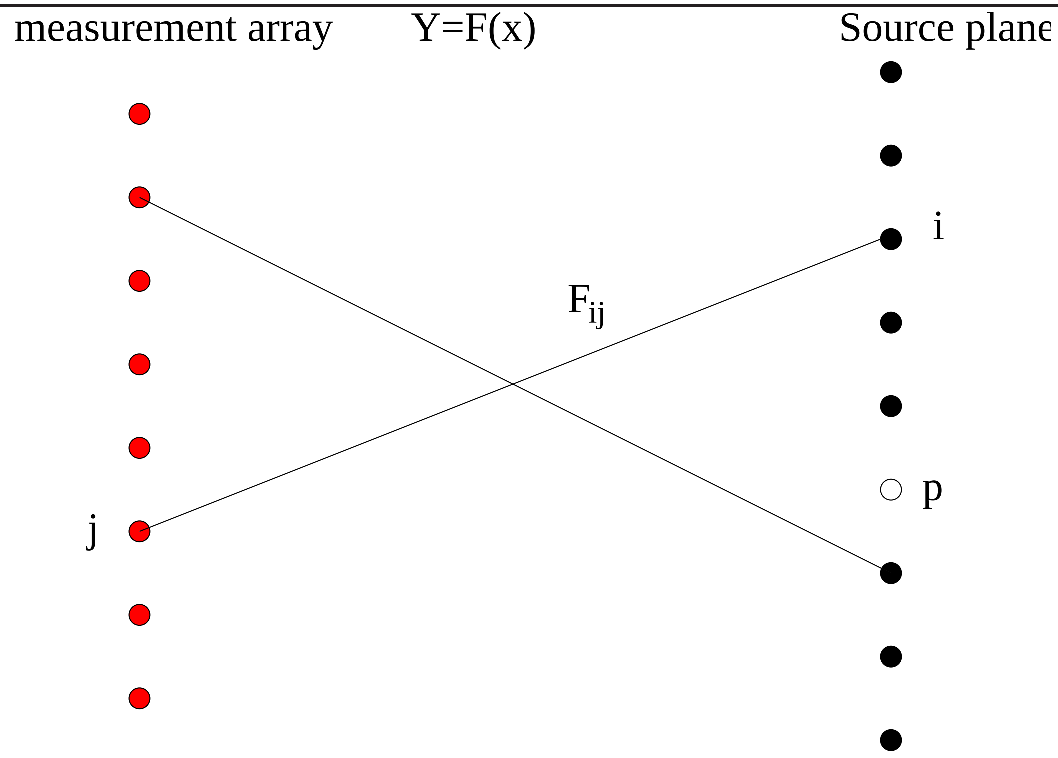

A point source fires at p. Given the measurement

$$\boldsymbol{y} = F(\boldsymbol{x}_m), \qquad \boldsymbol{x}_m = [0, \ldots, 1, \ldots, 0]^T$$

how to locate the source. Assume F is reciprocal.

Approximate F^{-1} and $\boldsymbol{x} = F^{-1}\boldsymbol{y}$

Assume $F = \{F_{ij}\}_{m\times n}$ is a linear operator and under-determined, $(m < n)$. The singular value decomposition of F is:

$$F = U_{m\times m} D_{m\times n} V^*_{n\times n}, \qquad D = diag(\lambda_1, \ldots, \lambda_m).$$

The least square solution is

$$\tilde{\boldsymbol{x}} = F^*(FF^*)^{-1}\boldsymbol{y} = VD^{-1}U^*\boldsymbol{y} = VV^*\boldsymbol{x}$$

• If D is close to singular, the inversion is sensitive to noise. Threshholding is needed.

$$\tilde{\boldsymbol{x}} = V^* diag(\frac{1}{\lambda_1}, \ldots, \frac{1}{\lambda_N}, 0, \ldots, 0)U^*\boldsymbol{y} = V^* diag(1, \ldots, 1, 0, \ldots, 0)V\boldsymbol{x}$$

which is the projection of $\boldsymbol{x}$ in the top N singular vectors.

• There is no nature way to implement F^{-1} and has to be approximated.

Time reverse the measurement y and send it back.
Assume spatial reciprocity $F_{ij} = F_{ji}$,

$$F^t\overline{\boldsymbol{y}} = F^t\overline{F\boldsymbol{x}} = \overline{V\,diag(\lambda_1^2, \ldots, \lambda_m^2)V^*\boldsymbol{x}}$$

• The time reveresal is robust.

• In physical time reversal F^t is naturally provided by the medium. In passive time reversal, e.g., target detection, F^t has to be approximated.

• Even F is nonlinear, the procedure can still be applied.

• Good for finding dominant events.

• Iterated time reversal ($\approx$ power method) can be used to find V for passive source.

Probing medium properties from scattered wave field.

Example, the harmonic wave field $u(\boldsymbol{x})$ satisfies

$$\Delta u(\boldsymbol{x}) + k^2 n(\boldsymbol{x}) u = f(\boldsymbol{x}),$$

where k is the wave number, $n(\boldsymbol{x})$ is the index of refraction, and $f(\boldsymbol{x})$ is the source (usually at the boundary).

- General inverse problem: find $n(\boldsymbol{x})$ inside a region from boundary data.

- Geometric approach: when $n(\boldsymbol{x})$ is piecewise constant find the interface where $n(\boldsymbol{x})$ jumps, i.e., the shape of scatterers, from boundary data.

The inverse problem is nonlinear!

Imaging methods

- Iterative methods: linearize the problem and make incremental improvement to match the measurement data.
  - pros: may find more detailed and accurate information.
  - cons: expensive and may not converge.
- Direct imaging methods: identify and visualize dominant information or physical quantities, such as location and boundary of target, directly.
  Key point: Need to understand the forward problem better and be able to extract information from the data.
  - pros: efficient and robust.
  - cons: may only recover partial information.

Our algorithm

A direct imaging method for extended target that uses

- a physical factorization of the scattering operator.

- a thresholding based on physical resolution.

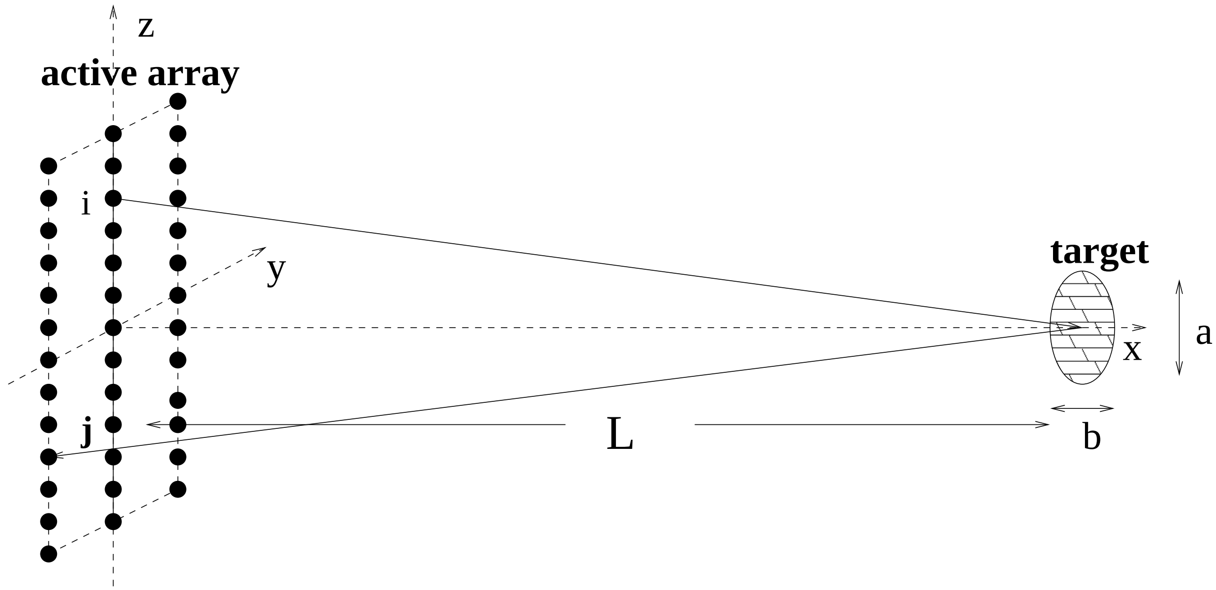

Define the *response matrix* $P = \{P_{ij}\}_{N\times N}$, where P_{ij} is the received signal at j-th transducer for a pulse sent out at i-th transducer and N is the number of transducers.

Remark: $P^H P$ is the time reversal matrix. Iterative time reversal is equivalent to the power method for finding the eigenvectors.

Imaging using an active array

- Structure and SVD pattern for the response matrix of an active array.

- Imaging using SVD of the response matrix.

- Target Detection and Imaging in random medium.

Point targets

For M point targets at $\boldsymbol{y}_m$ with reflectivity τ_m,

$$P_{ij}(k) = \sum_{m=1}^{M} \tau_m G(\boldsymbol{x}_i, \boldsymbol{y}_m) G(\boldsymbol{x}_j, \boldsymbol{y}_m) \quad \Rightarrow \quad P(k) = \sum_{m=1}^{M} \tau_m \vec{g}_m \vec{g}_m^T$$

The eigenspace of the response matrix is spanned by $\{\vec{g}_1, \ldots, \vec{g}_M\}$.
$G(\boldsymbol{x}, \boldsymbol{y})$ is the Green's function and $\vec{g}_m$ is the illumination vector:

$$\vec{g}_m = [G(\boldsymbol{x}_1, \boldsymbol{y}_m), G(\boldsymbol{x}_2, \boldsymbol{y}_m), \ldots, G(\boldsymbol{x}_N, \boldsymbol{y}_m)]^T$$

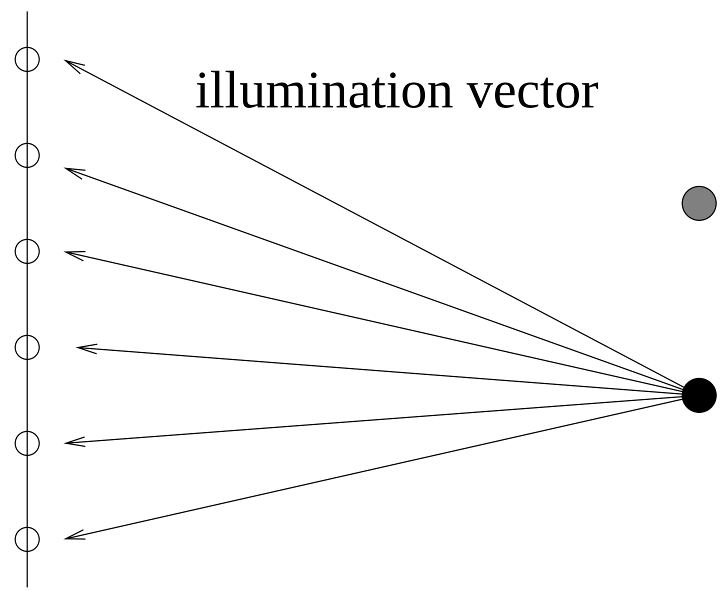

If the targets are well resolved by the active array, i.e, the time reversal resolution can distinguish different targets, the point spread function

$$\Gamma(\boldsymbol{x}_m, \boldsymbol{x}_{m'}) = \overline{\vec{g}_m^T} \vec{g}_{m'} \approx 0 \qquad \text{if } m \neq m'.$$

The singular vectors are $\vec{g}_m$, i.e., there is a 1-to-1 correspondence

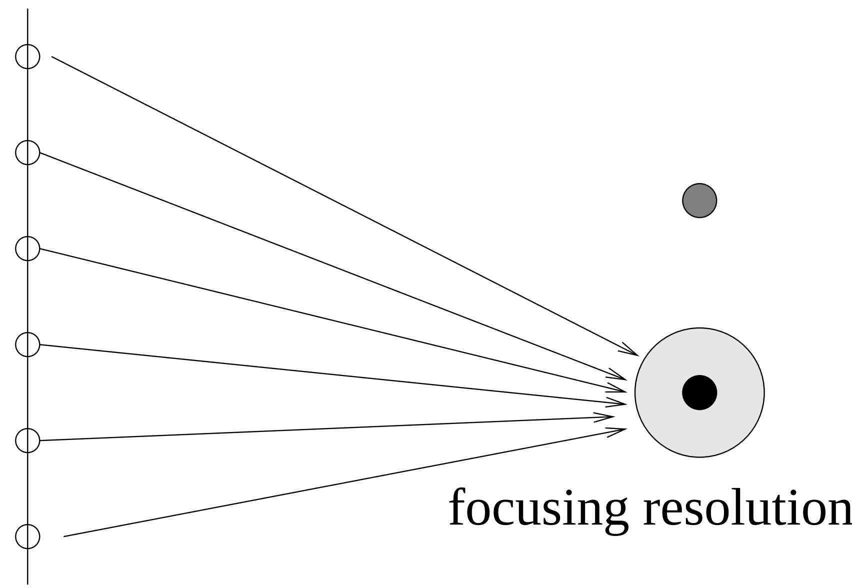

Extended targets

In general the response matrix for a single extended target can have a continuous spectrum.

Denote:

- L the distance between the array and the target,
- λ the wave length,
- s the characteristic dimension of the target,
- a the size of the array,

The number of significant singular values and vectors of the response matrix is $\propto \frac{s}{R_t}$ where R_t is the time reversal focusing resolution. In the remote sensing regime, $R_t = \frac{\lambda L}{a}$.

Pattern for the SVD of the response matrix

- Point targets ($s \ll R_t$): the rank of the response matrix is equal to the number of targets; each singular vector is a combination of the illumination vectors, i.e., contains only location information.

- Small targets ($s < R_t$): grouped singular values; SVD can reveal both location and size (moment) information of the targets. (Chambers; Zhao)

- Large targets ($s \geq R_t$): a continuous spectrum that contains both location and geometry information of the target.

The spectrum for an extended (small) target.

- the dominant singular vector is rg

  $$\vec{g} = [G(\boldsymbol{\xi}_1, \boldsymbol{o}), G(\boldsymbol{\xi}_2, \boldsymbol{o}), \ldots, G(\boldsymbol{\xi}_N, \boldsymbol{o})]^T$$

  with singular value $|\lambda_1| \approx |\Omega||\vec{\vec{g}}|^2$

- the next two dominant eigenvectors:

  $$\vec{g}_y = [G_y(\boldsymbol{\xi}_1, \boldsymbol{o}), G_y(\boldsymbol{\xi}_2, \boldsymbol{o}), \ldots, G_y(\boldsymbol{\xi}_N, \boldsymbol{o})]^T$$

  with singular value $|\lambda_2| \approx \frac{k^2}{L^2}|\vec{g}_y|^2 \int_\Omega y^2$,

  $$\vec{g}_z = [G_z(\boldsymbol{\xi}_1, \boldsymbol{o}), G_z(\boldsymbol{\xi}_2, \boldsymbol{o}), \ldots, G_z(\boldsymbol{\xi}_N, \boldsymbol{o})]^T$$

  with singular value $|\lambda_3| \approx \frac{k^2}{L^2}|\vec{g}_z|^2 \int_\Omega z^2$

$\boldsymbol{\xi}_i = (L, \eta_i, \zeta_i)$ is the position of the ith transducer; $\boldsymbol{o}$ is the center of the target.

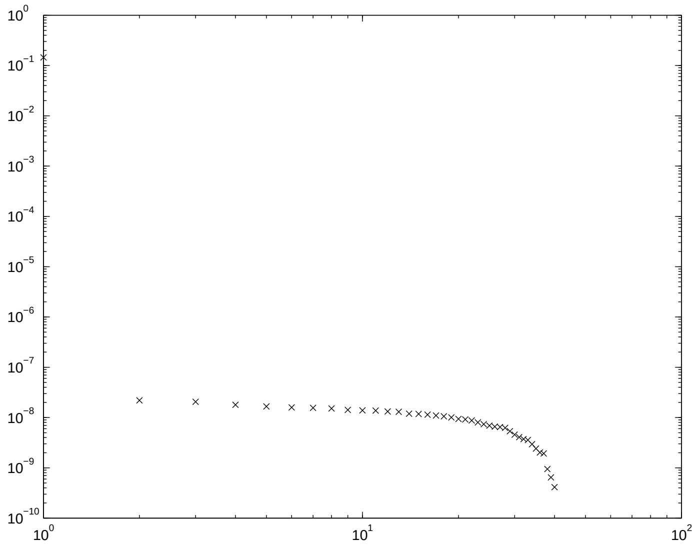

(a) point target ($s = 0.05\lambda$)

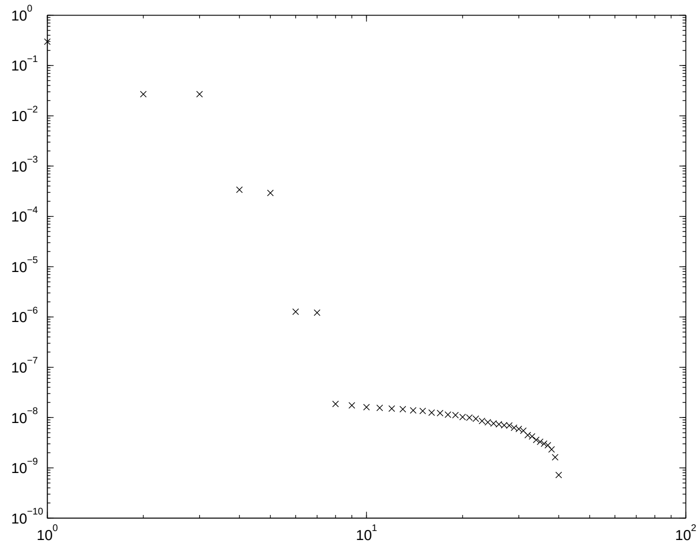

(b) small extended target ($s = 0.3\lambda$)

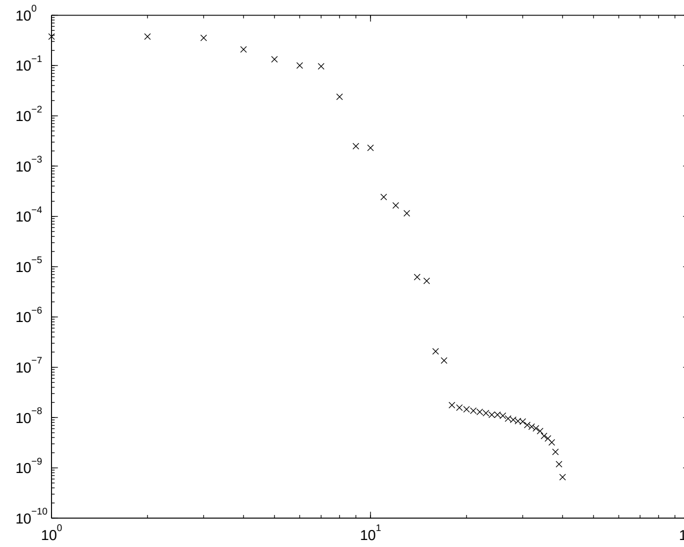

(c) extended target ($s = 2.5\lambda$)

Imaging algorithm for point targets

MUltiple SIgnal Classification (Schmidt, Devaney) is an algorithm for imaging point targets in a known background when *the number of targets is smaller than the number of transducers*.

Even with multiple scattering among the targets the response matrix can be factorized as

$$P_{ij}(k) = \sum_{m=1}^{M} \tau_m G^0(\boldsymbol{x}_i, \boldsymbol{y}_m) G(\boldsymbol{x}_j, \boldsymbol{y}_m) \quad \Rightarrow \quad P(k) = \sum_{m=1}^{M} \tau_m \vec{g}_m^{\,0} \vec{g}_m^{\,T}$$

G^0 is the Green's function for the background and G is the Green's function that includes multiple scattering among targets.

The column space V_s of the response matrix is still spanned by $\{\vec{g}_1^{\,0}, \ldots, \vec{g}_M^{\,0}\}$.

Imaging function: $\Phi(\boldsymbol{x}) = \|(I - P_{V_S})\vec{g}^{\,0}(\boldsymbol{x})\|^{-1}$,
where P_{V_S} is the projection to the signal space V_s.

SVD of the response matrix in homogeneous medium with two targets.

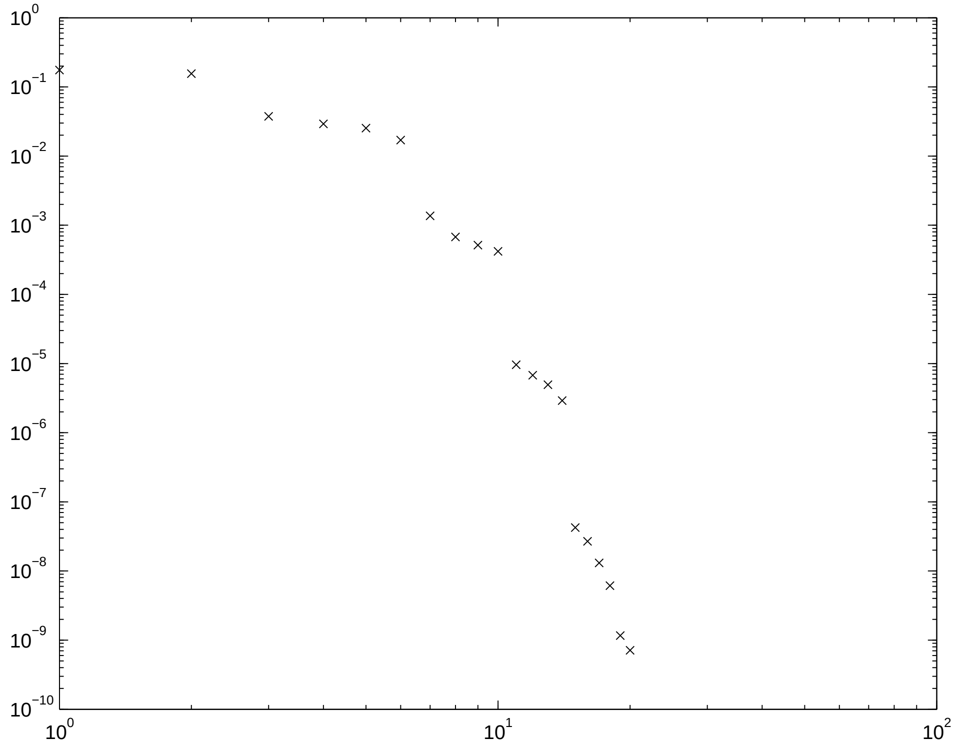

(a) singular values

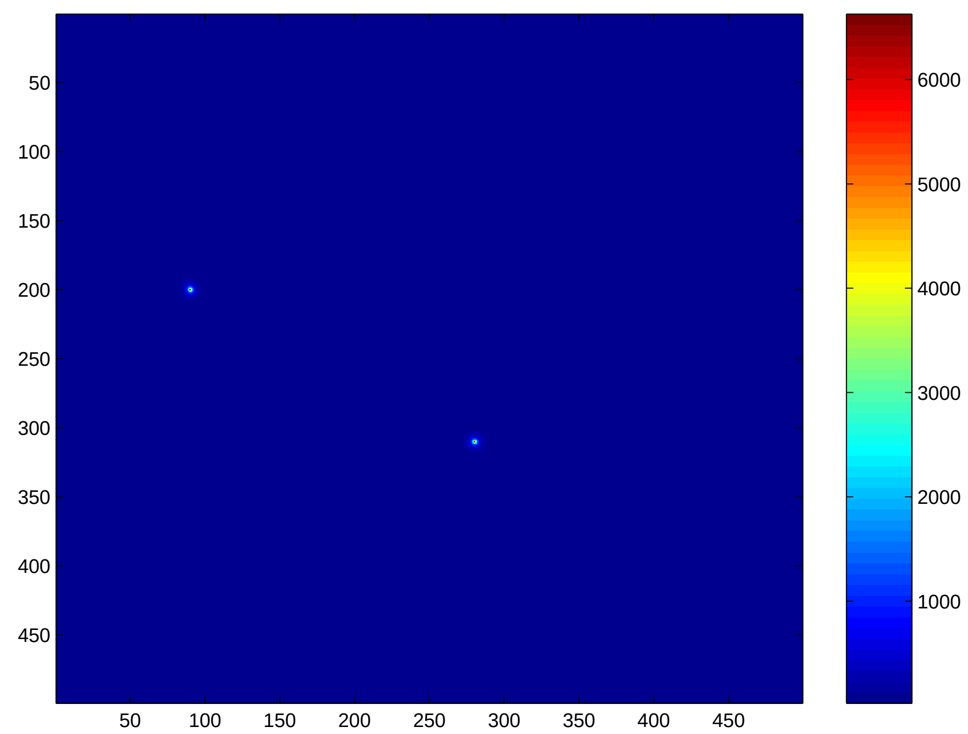

(c) MUSIC

If the target size s is larger or comparable to the array resolution r, the response matrix will have a set of significant singular values and singular vectors. The space spanned by the corresponding singular vectors is defined as the shape space V_s. The dimension is proportional to $\frac{s}{r}$.

We define the imaging function as

$$\Phi(\boldsymbol{x}) = \|(I - P_{V_S})\vec{g}(\boldsymbol{x})\|^{-1}$$

Key point: What is the shape space and how to define the illumination vector $\vec{g}(\boldsymbol{x})$ based on factorization of the scattering operator,

Remark: Each signular vector does not correspond to an illumination vector, i.e., an extended target can not be viewed as a collection of point targets.

Dirichlet boundary condition

The scattered field u^s for a perfect conductor ($u = 0$ at $\partial\Omega$) with the incident field u^i is

$$u^s(\boldsymbol{x}) = \int_{\partial\Omega} \frac{\partial G(\boldsymbol{x}, \boldsymbol{y})}{\partial\nu} u^i(\boldsymbol{y}) d\boldsymbol{y},$$

where $G(x, y)$ is the (**unknown**) Green's function with the scatterer. The response matrix becomes

$$P_{ij} = \int_{\partial\Omega} \frac{\partial G(\boldsymbol{x}_j, \boldsymbol{y})}{\partial\nu} G_0(\boldsymbol{x}_i, \boldsymbol{y}) d\boldsymbol{y}$$

where $\boldsymbol{x}_i$ is the i-th transducer. The matrix can be factorized as

$$P = \int_{\partial\Omega} \vec{g}_0(\boldsymbol{y}) \left[\frac{\partial \vec{g}(\boldsymbol{y})}{\partial\nu}\right]^T d\boldsymbol{y}$$

$\vec{g}_0(y)$ and $\vec{g}(y)$ are the illumination vectors in the homogeneous and inhomogeneous medium respectively. The sources for the scattered field are monopoles at the boundary parts that are well illuminated by the array and should be in the signal space of the response matrix, i.e., $\vec{g}_0(\boldsymbol{y}) \in V_s$, for $\boldsymbol{y}$ on the well illuminated parts of the boundary.

Let $\vec{u}_i$ be the singular vectors with singular values σ_i. Define the signal space $V_s = span\{\vec{u}_i | \, |\sigma_i| > n\}$, where n is a threshhold depending on the resolution of the array and noise level. We use illumination vector $\vec{g}(\boldsymbol{x}) = [G_0(\boldsymbol{x}_1, \boldsymbol{x}), \ldots, G_0(\boldsymbol{x}_N, \boldsymbol{x})]^T$. The imaging function

$$\Phi(\boldsymbol{x}) = \|(I - P_{V_S})\vec{g}(\boldsymbol{x})\|^{-1}$$

will peak at the boundary.

Remark: Although the signal space is $\approx$ spanned by the illumination vectors on the well illuminated boundary. However the boundary integral operator with unknown kernel G makes the SVD complicated. **Each singular vector does not correspond to an illumination of a point target on the boundary.**

Imaging extended targets with Dirichlet BC

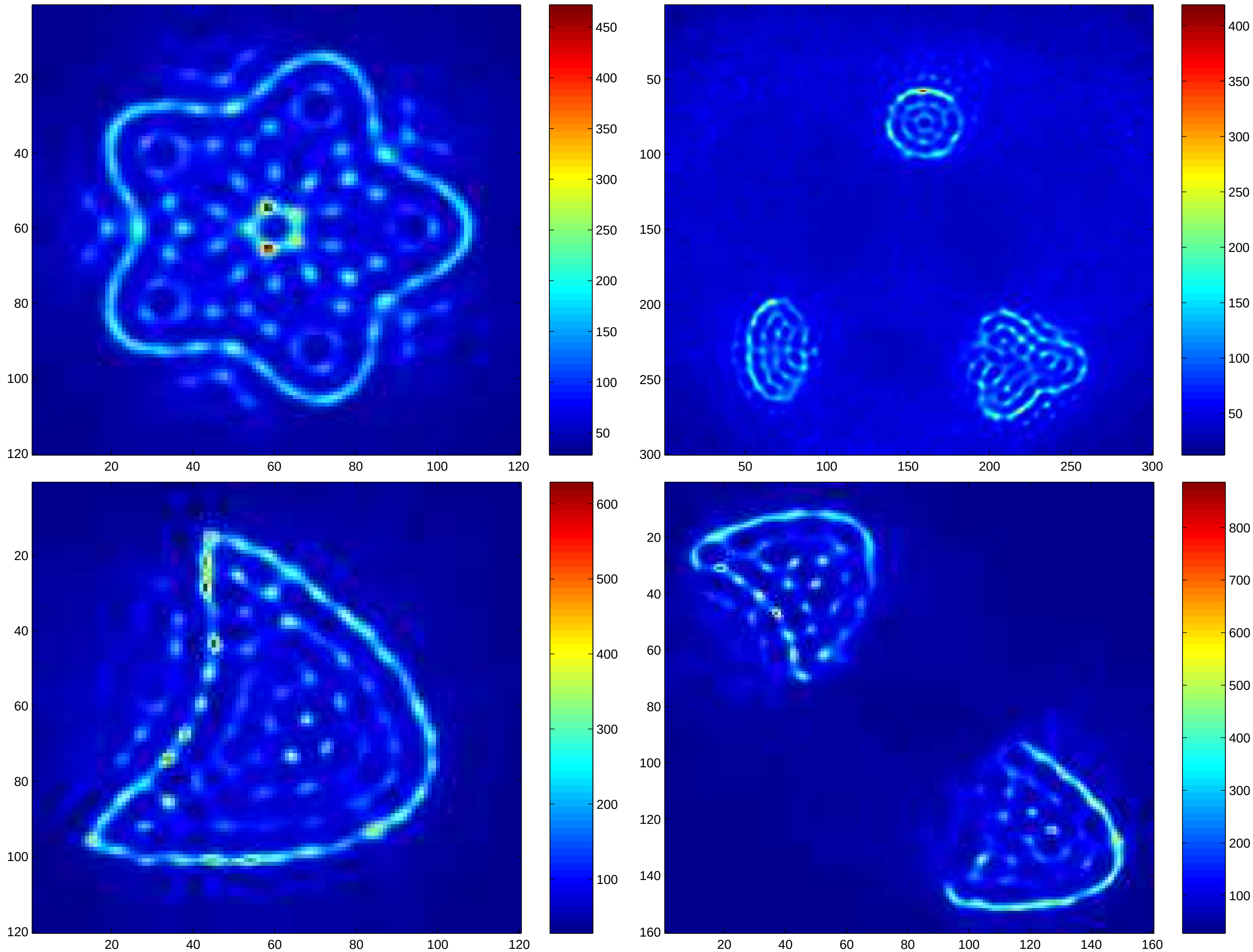

80 transducers surround the targets. $\lambda = 16h$, Distance $= 200h$.

The scattered field u^s for a perfect reflector ($\frac{\partial u}{\partial n} = 0$ at $\partial\Omega$) with the incident field u^i is,

$$u^s(\boldsymbol{x}) = \int_{\partial\Omega} G(\boldsymbol{x}, \boldsymbol{y}) \frac{\partial u^i(\boldsymbol{y})}{\partial \nu} d\boldsymbol{y}$$

the response matrix for the scattered field is

$$P_{ij} = \int_{\partial\Omega} G(\boldsymbol{x}_j, \boldsymbol{y}) \frac{\partial G_0(\boldsymbol{x}_i, \boldsymbol{y})}{\partial \nu} d\boldsymbol{y}$$

$\boldsymbol{x}_i$ is the i-th transducer. The matrix can be factorized as

$$P = \int_{\partial\Omega} \frac{\partial \vec{g}_0(\boldsymbol{y})}{\partial \nu} \vec{g}^T(\boldsymbol{y}) d\boldsymbol{y}$$

$\vec{g}_0(y)$ and $\vec{g}(y)$ are the illumination vectors in the homogeneous and inhomogeneous medium respectively. The sources for the scattered field are dipoles at the boundary parts that are well illuminated by the array and should be in the signal space of the response matrix, i.e., $\frac{\partial \vec{g}_0(\boldsymbol{y})}{\partial \nu} \in V_s$, for $\boldsymbol{y}$ on the well illuminated parts of the boundary.

We define a signal space V_s based on the SVD of the response matrix and use dipole

$$\vec{g}(\boldsymbol{x}) = [\frac{\partial G_0(\boldsymbol{x}_1, \boldsymbol{x})}{\partial \nu_k}, \ldots, \frac{\partial G_0(\boldsymbol{x}_N, \boldsymbol{x})}{\partial \nu_k}]^T$$

as illumination vector, where ν_k is in a set of fixed discrete directions. The imaging function is

$$\Phi(\boldsymbol{x}) = \left[\min_{\nu_k} \| (I - P_{V_S}) \vec{g}(\boldsymbol{x}) \| \right]^{-1}$$

Imaging extended target with Neumann boundary condition

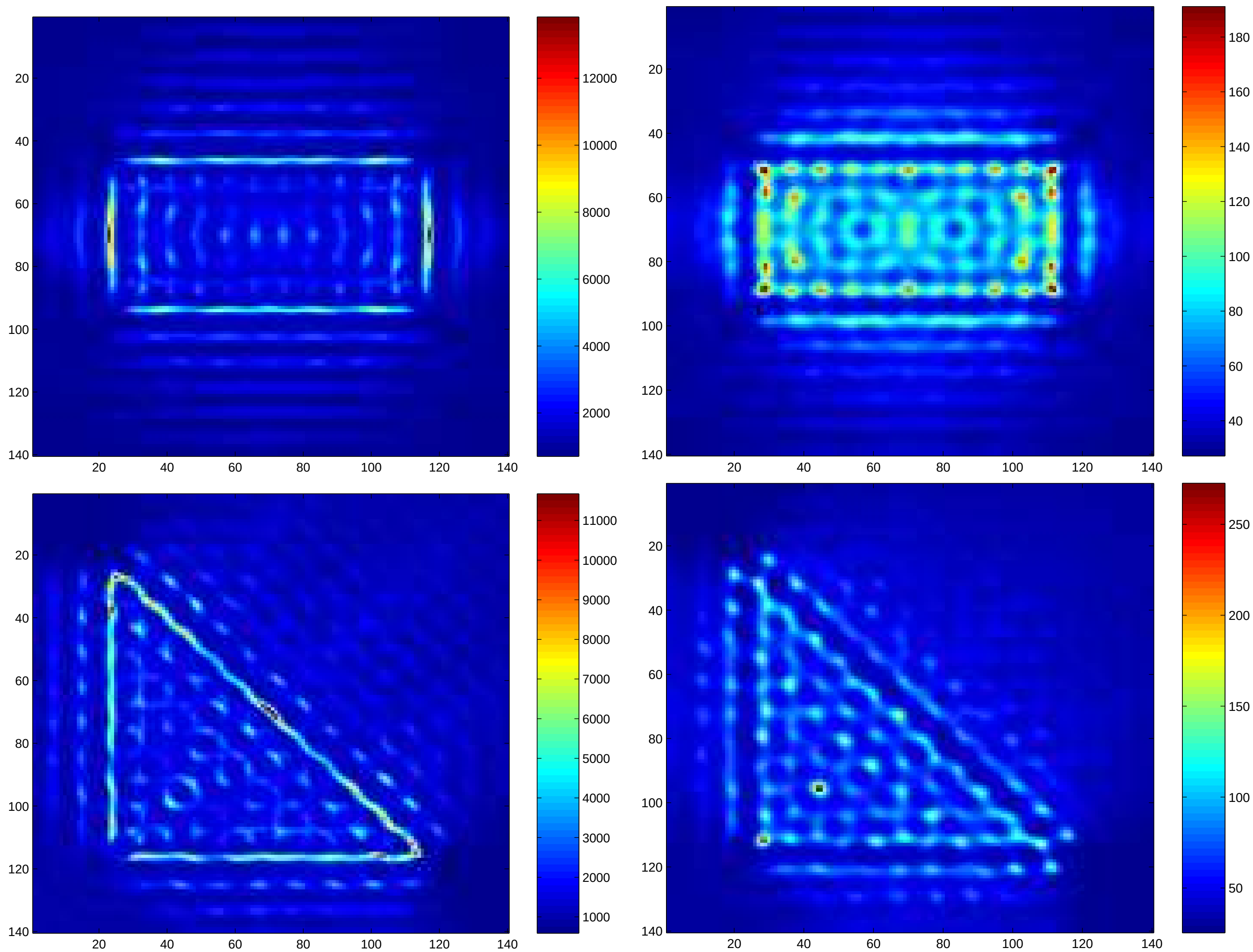

use dipole as illumination vector use monopole as illumination vector

Using wrong illuminination vectors

Neumann boundary condition with Dirichlet imaging function

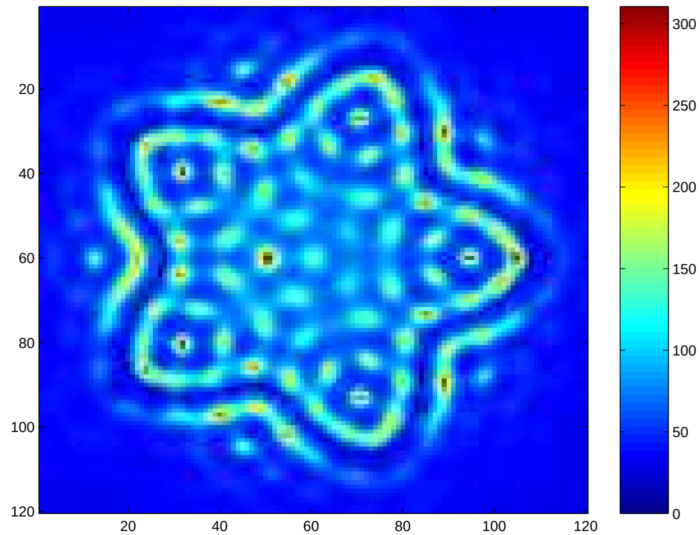

Dirichlet boundary condition with Neumann imaging function

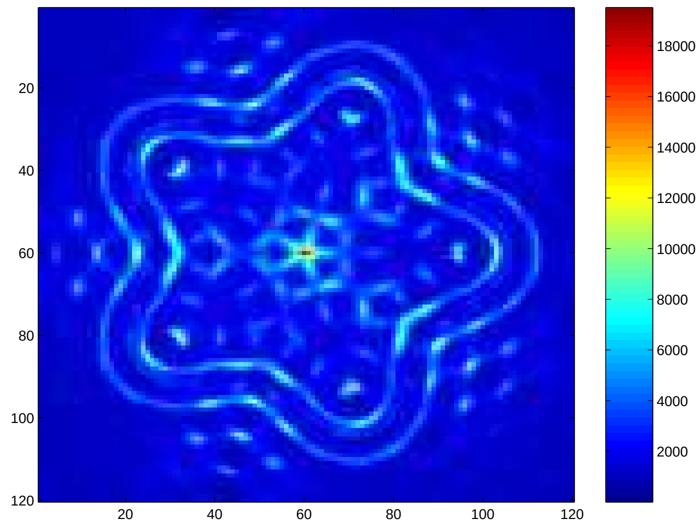

If $\frac{\partial u}{\partial \nu} + i\mu u = 0$ on the target boundary, we have the following integral equation:

$$u^s(x) = \int_{\partial D} \frac{\partial u^i(y)}{\partial \nu} G(\boldsymbol{x}, \boldsymbol{y}) - \frac{\partial G(\boldsymbol{x}, \boldsymbol{y})}{\partial \nu} u^i(y) dS(y) \tag{1}$$

Using the boundary condition we have

$$u^s(x) = \int_{\partial D} \left[i\mu u^i(\boldsymbol{y}) + \frac{\partial u^i(\boldsymbol{y})}{\partial \nu} \right] G(\boldsymbol{x}, \boldsymbol{y}) d\boldsymbol{y} \tag{2}$$

So the response matrix is of the form

$$P = \int_{\partial \Omega} \left[i\mu \vec{g}_0(\boldsymbol{y}) + \frac{\partial \vec{g}_0(\boldsymbol{y})}{\partial \nu} \right] \vec{g}^T(\boldsymbol{y}) d\boldsymbol{y}$$

If we know μ we should use a combination of monopole and dipole as illumination vector.

Imaging extended targets with Robin boundary condition

$\mu = 0.2$ (Neumann like)

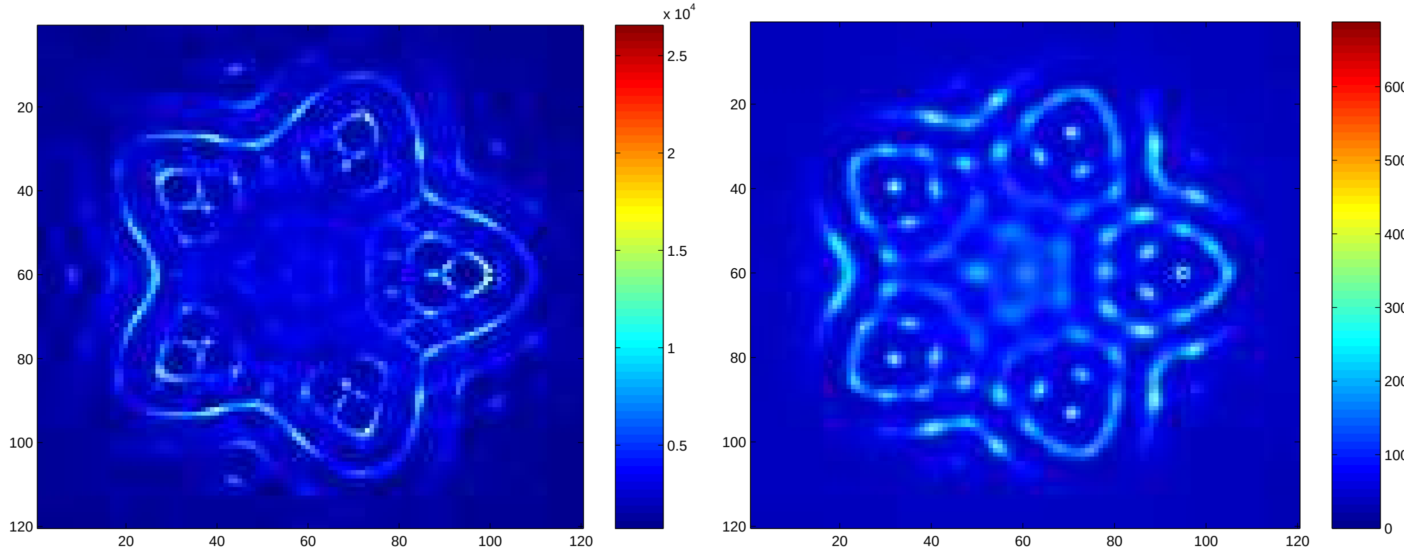

$\mu = 2$ (Dirichlet like)

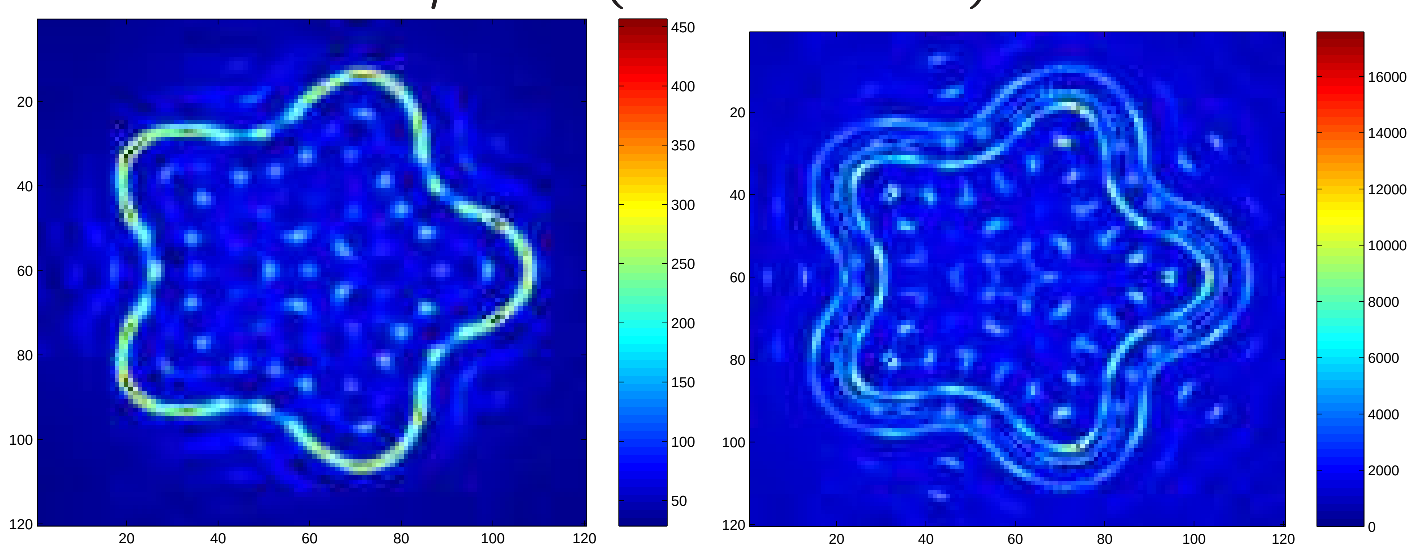

use dipole as illumination vector use monopole as illumination vector

Mixed boundary condition (partially coated target)

If a target has a mixed boundary condition, i.e., part of the boundary has Dirichlet or Dirichlet-like Robin condition, part of the boundary has Neumann or Neumann-like Robin condition. Our algorithm can identify different parts using different type of illumination vectors.

For example, a metal tank is partially coated by dielectric to avoid radar detection, our algorithm can tell which part of the boundary is metal and which part is dielectric.

The upper half of the object has $\mu = 0.2$(Neumann-like) and the lower half of the object has $\mu = 2$(Dirichlet-like).

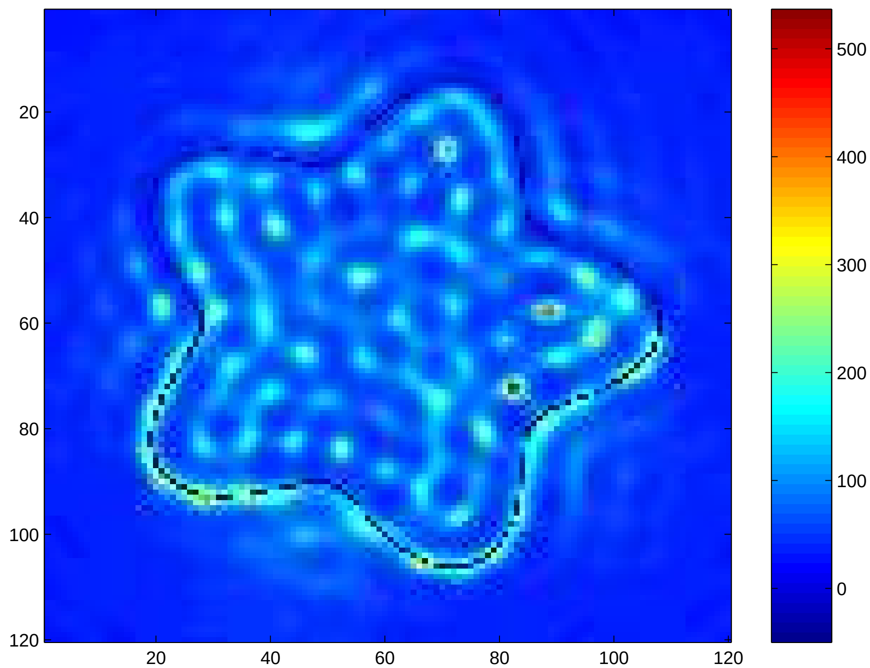

use dipole as illumination vector

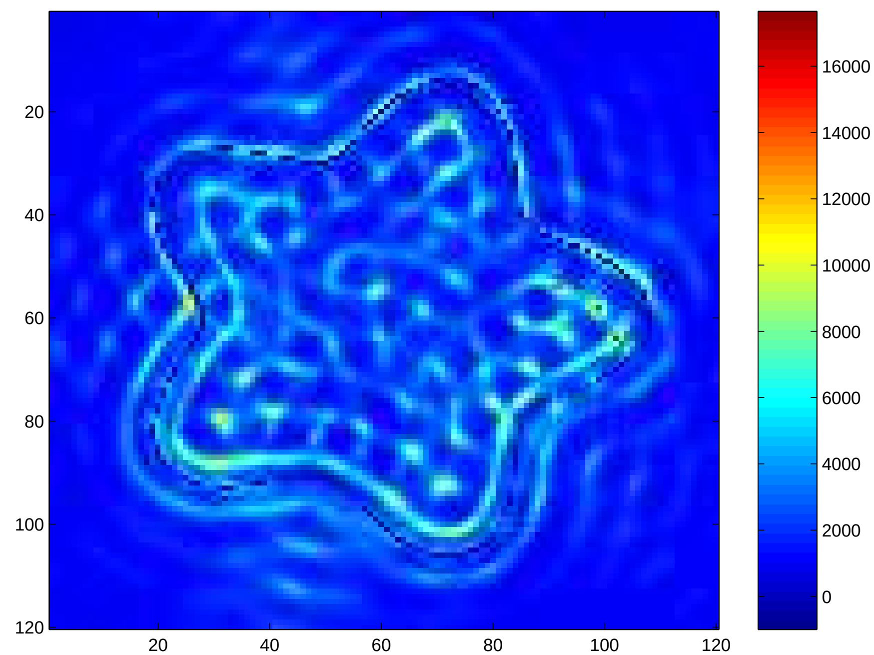

use monopole as illumination vector

Penetrable targets

For a smooth varying contrast σ with compact support Ω,

$$u(\boldsymbol{x}) = u^i(\boldsymbol{x}) + \int_\Omega G_0(\boldsymbol{x}, \boldsymbol{y})\sigma(\boldsymbol{y})u(\boldsymbol{y})dy$$

The response matrix for the scattered field is

$$P_{ij} = \int_\Omega \sigma(\boldsymbol{y})G_0(\boldsymbol{x}_i, \boldsymbol{y})G(\boldsymbol{x}_j, \boldsymbol{y})dy,$$

The matrix form is

$$P = \int_\Omega \sigma(\boldsymbol{y})\vec{g}_0(\boldsymbol{y})\vec{g}^T(\boldsymbol{y})d\boldsymbol{y}$$

The sources are located inside the support.

Imaging function will peak inside the region.

$$u(\boldsymbol{x}) = u^i(\boldsymbol{x}) + \int_{\partial\Omega} \frac{\partial G_0(\boldsymbol{x},\boldsymbol{y})}{\partial\nu(\boldsymbol{y})}\psi(\boldsymbol{y}) + G_0(\boldsymbol{x},\boldsymbol{y})\phi(\boldsymbol{y})d\boldsymbol{y}$$

where ϕ and ψ are density functions for single and double layer potentials. The response matrix is

$$P_{ij} = \int_{\partial\Omega} \frac{\partial G_0(\boldsymbol{x}_j,\boldsymbol{y})}{\partial\nu(\boldsymbol{y})}\psi(\boldsymbol{x}_i,\boldsymbol{y}) + G_0(\boldsymbol{x}_j,\boldsymbol{y})\phi(\boldsymbol{x}_i,\boldsymbol{y})d\boldsymbol{y}$$

The matrix form is

$$P = \int_{\partial\Omega} \frac{\partial \vec{g}_0(\boldsymbol{y})}{\partial\nu(\boldsymbol{y})}\vec{\psi}^T(\boldsymbol{y}) + \vec{g}_0(\boldsymbol{y})\vec{\phi}^T(\boldsymbol{y})d\boldsymbol{y}$$

Again the sources are monopoles and dipoles located at the boundary parts that are well illuminated by the array.

Imaging function will peak at or near the boundary.

Imaging penetrable extended targets

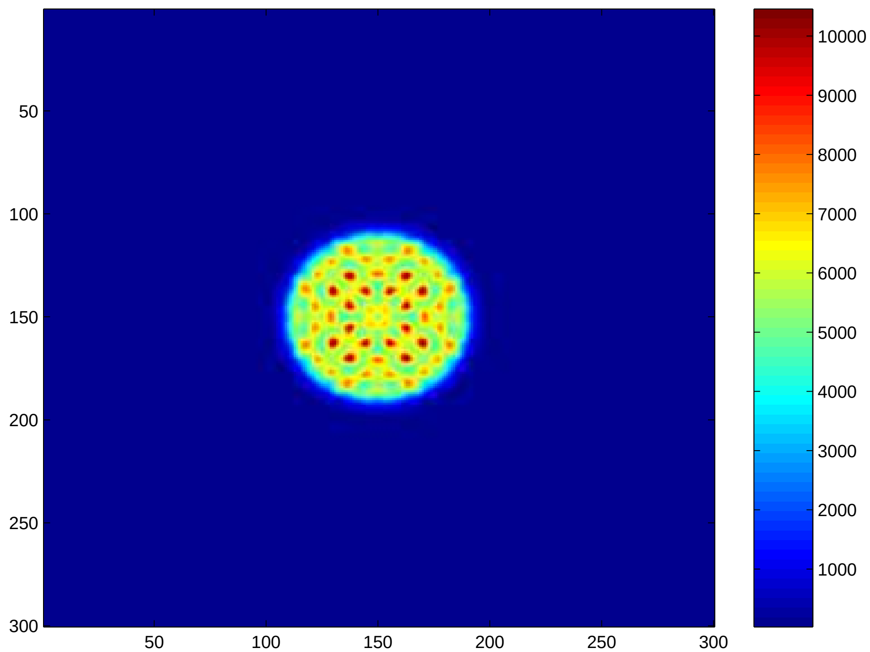

(a) smooth variation

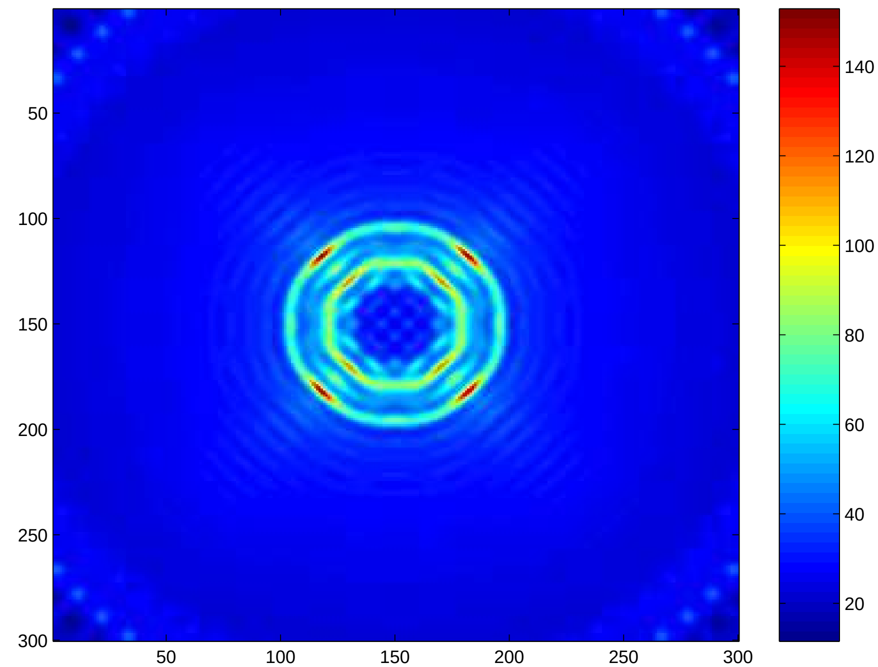

(b) constant contrast

a target with the shape of three leaves (comparable to wavelength) and finite contrast

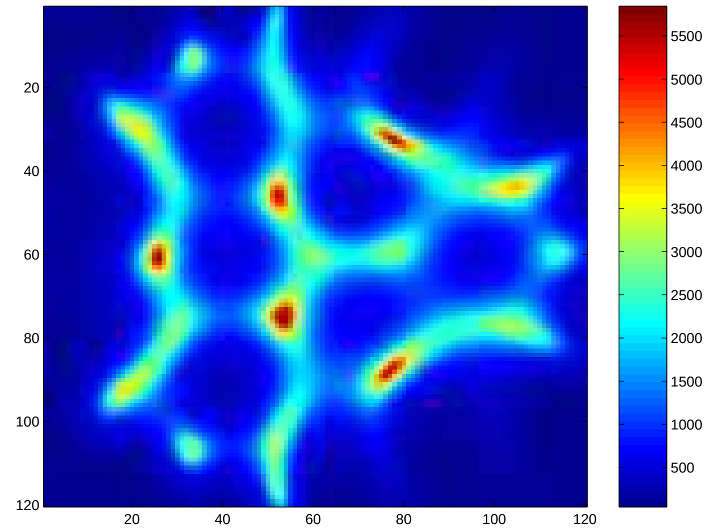

2 circular targets with smooth transition of contrast

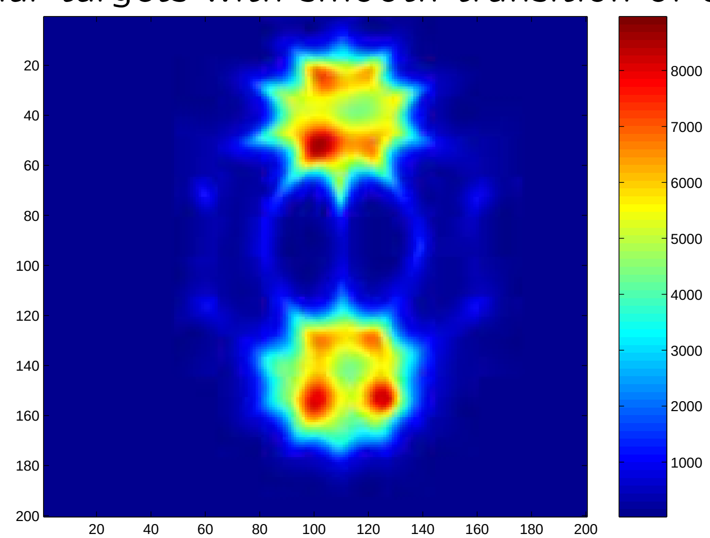

Let s be the size of the target and r be the resolution of the array. the number of significant singular values and singular vectors is $\propto \frac{s}{r}$

In the remote sensing regime $r \propto \frac{\lambda L}{a}$, L is the distance, λ is the wavelength, and a is the aperture of the array.

Let $\sigma_1 > \sigma_2 > \ldots > \sigma_N$ are the singular values for the response matrix and the signal space V^S is spanned by the first n singular vectors. Define the signal-to-noise ratio: $\frac{\|P_{signal}\|_2}{\|P_{noise}\|_2} = \frac{\sigma_1}{\sigma_{n+1}}$. We tested that $\frac{\sigma_1}{\sigma_{n+1}}$ depends only weakly on the parameters and the shape of the target(s). This criterion can be used to determine the threshold.

Shape space

80 transducers in total.

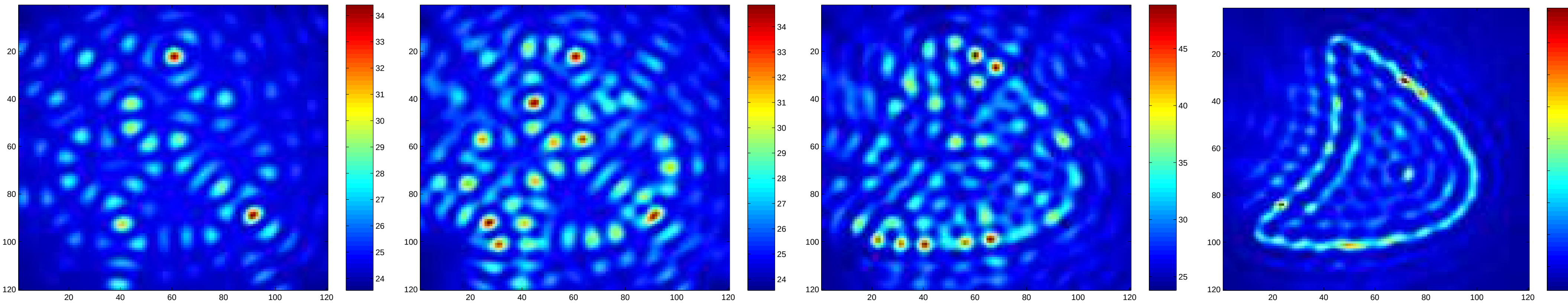

1 vector | 2 vectors | 5 vectors | 18 vectors

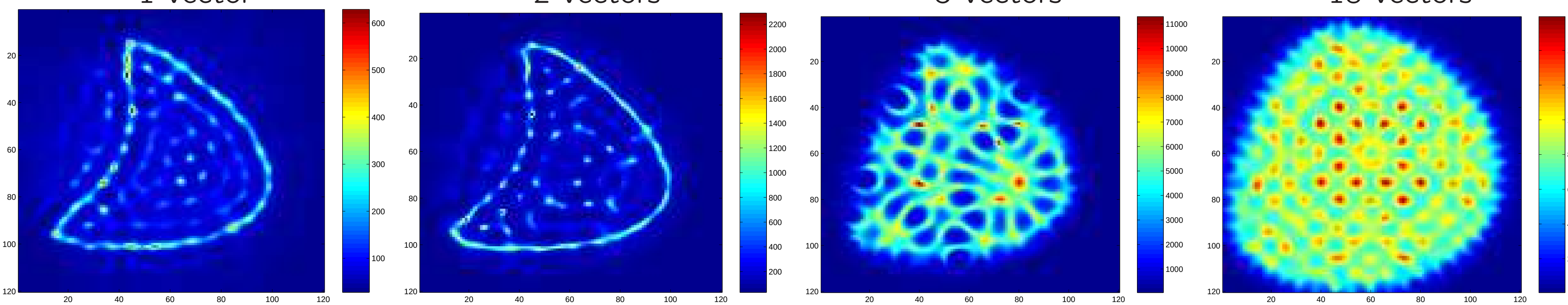

25 vector | 32 vectors | 40 vectors | 50 vectors

Geometry of the target with certain resolution is embeded in a subspace of the eigenspace of the response matrix.

A slide show in practice to reveal different structures.

40 transducers in total.

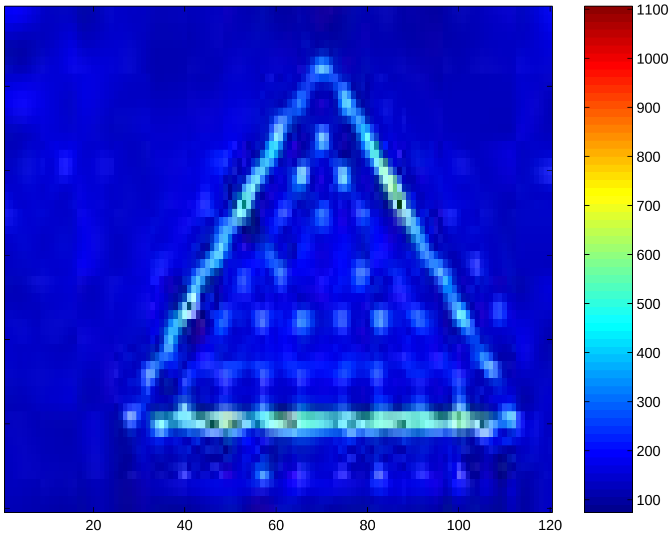

$\lambda = 12h$

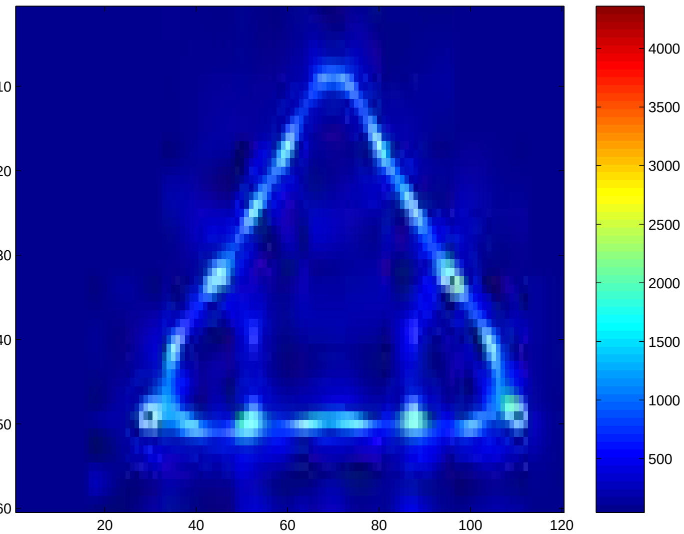

$\lambda = 24h$

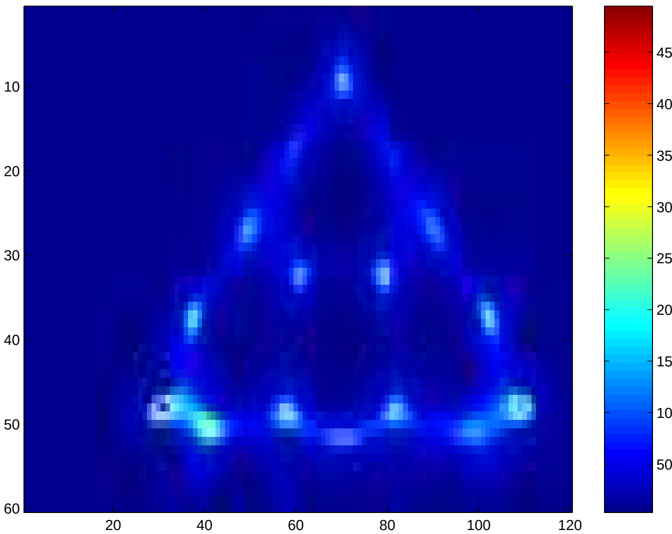

$\lambda = 32h$

Robustness with respect to noise

40 transducers.

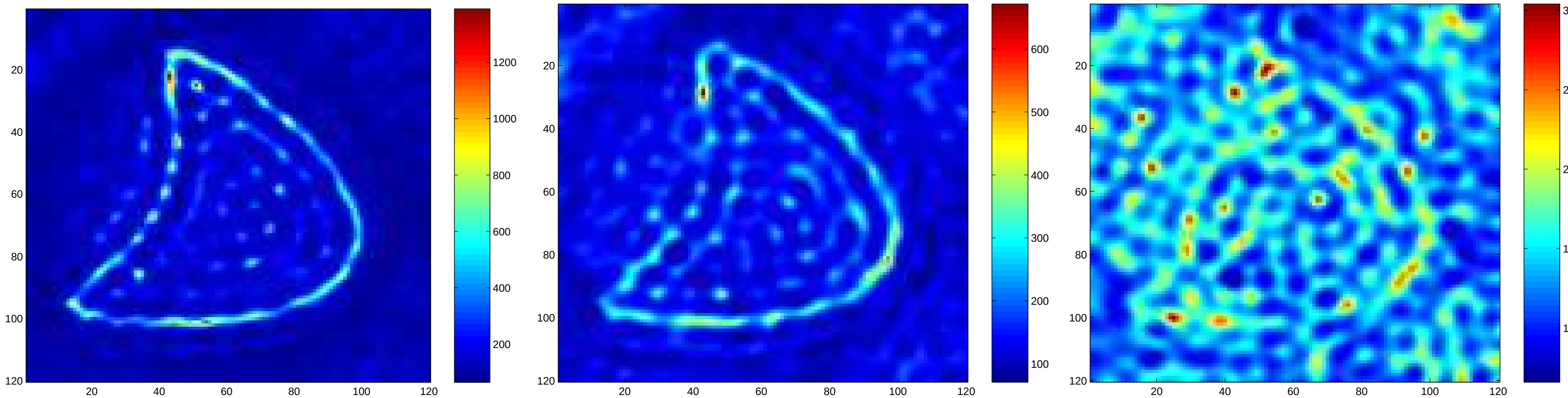

no noise | 100% noise | 200% noise

80 transducers.

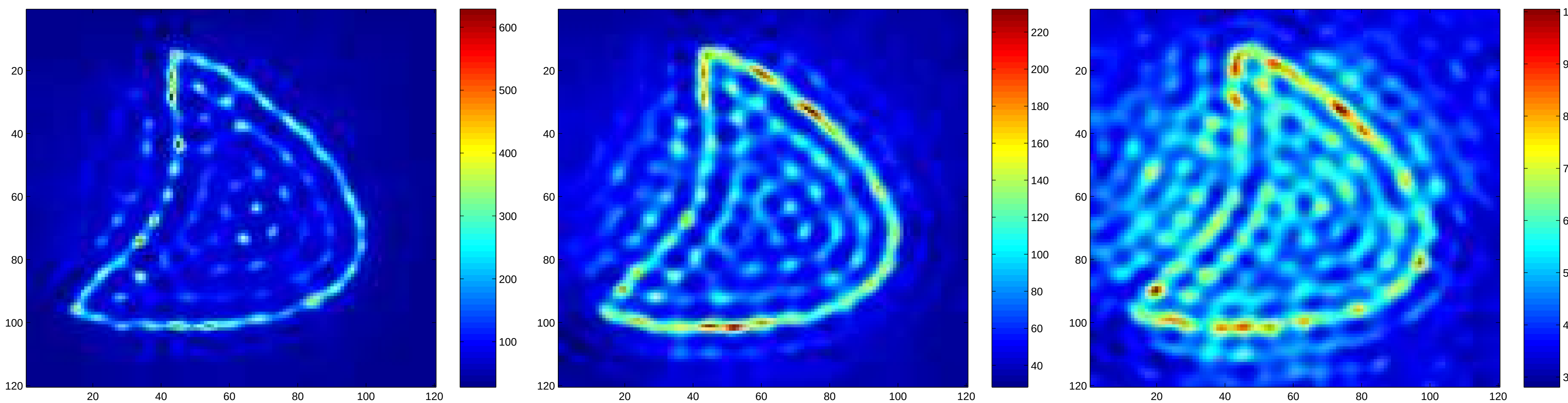

no noise | 100% noise | 200% noise

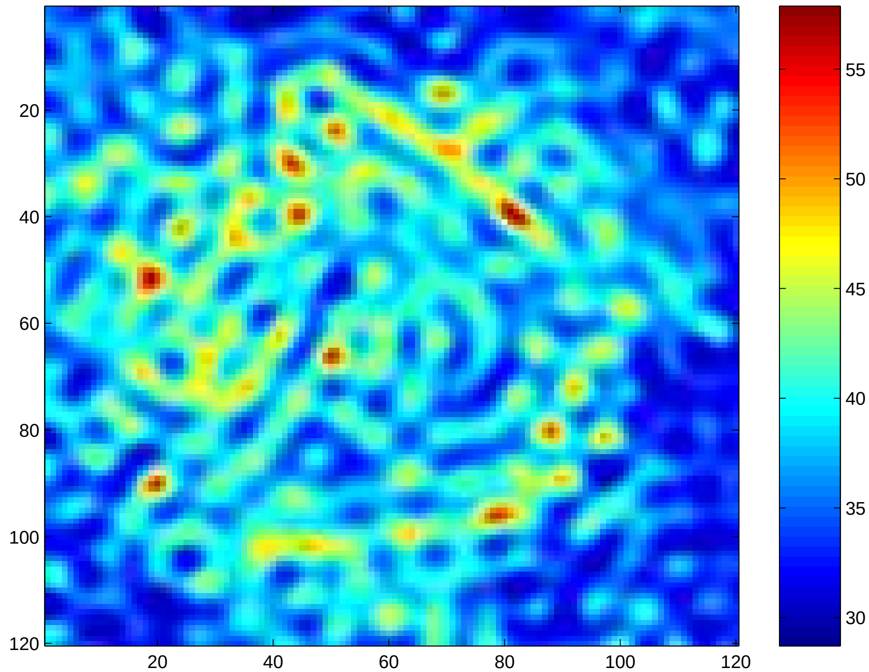

400% noise $\lambda = 16h$

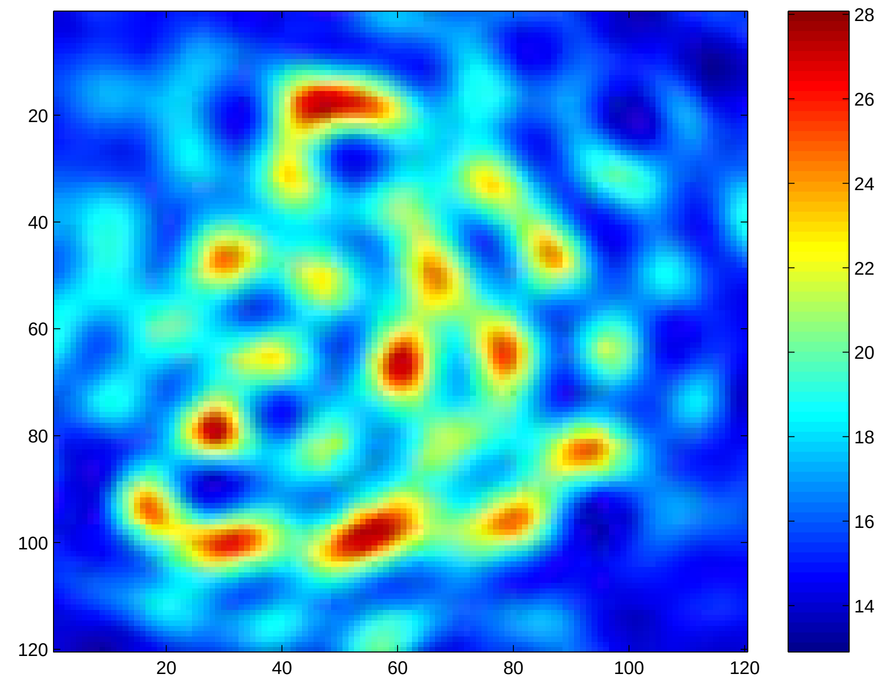

400% noise $\lambda = 32h$

Longer wavelength $\Rightarrow$ more robustness.

Linear sampling method (Colton and Kirsch 1996) is based on the far field scattering map (measured data) $F_\infty(\hat{x}, \hat{\theta}), \hat{x}, \hat{\theta} \in S^n$ due to a scatterer Ω. An incoming plane wave form $g(\hat{\theta})$ is mapped to a far field pattern: $u_\infty(\hat{x}) = \int_{S^n} F_\infty(\hat{x}, \hat{\theta}) g(\hat{\theta}) d\hat{\theta}$

It can be shown that if $\boldsymbol{z} \in \Omega$ then the far field pattern of a point source at $\boldsymbol{z}$ is in the range of F and there exists $g(\hat{\theta})$ such that $F(g)$ approximate $e^{-ik\hat{x}\cdot\boldsymbol{z}}$ well. Moreover $\|g\|_{L^2} \to \infty$ as $\boldsymbol{z} \to \partial\Omega$.

Later Kirsch (1998) show that the range of the far field map is the same as $(F^*F)^{1/4}$, i.e., $(F^*F)^{1/4} g = e^{-ik\hat{x}\cdot\boldsymbol{z}}$ is solvable iff $\boldsymbol{z} \in \Omega$. Let λ_j, ψ_j be the eigensystem of F and $\rho_j(\boldsymbol{z}) = < e^{-ik\hat{x}\cdot\boldsymbol{z}}, \psi_j >$,

$$\boldsymbol{z} \in \Omega \quad \text{iff} \quad \sum \frac{|\rho_j(\boldsymbol{z})|^2}{|\lambda_j|} < \infty$$

Comparison with linear sampling method

- Different factorization.
- Same for near field or far field.
- Different imaging function for different physical boundary conditions.
- Thresholding (regularization) based on SVD and physical scales.

Target detection and imaging in heterogeneous medium

For heterogeneous medium: *the Green function is not known*. The response matrix contains information of both the medium and the targets. And inverse the whole medium is too expensive.

Key points:

- Separate the target signal from the background medium.
- Design statistical stable imaging function using multiple frequencies.
- Get better estimate of the Green function for the background medium using effective theory and available measurments.

Factorization for general model

The data contains both model error and measurement noise. For example, with Dirichlet BC,

$$P_{ij} = \int_{\partial\Omega} \frac{\partial G_T(\boldsymbol{x}_j, \boldsymbol{y})}{\partial \nu} G_B(\boldsymbol{x}_i, \boldsymbol{y}) d\boldsymbol{y} \text{ (+ or } \times\text{) measurement noise}$$

where G_T is the Green's function contains information of the target and G_B is the Green's function contains information of the background random medium.

- Measurement noise can be dealt with using SVD and thresh-holding.

- Random background can be dealt with using effective medium property and multiple-frequencies.

Some preliminary results using multiple frequencies

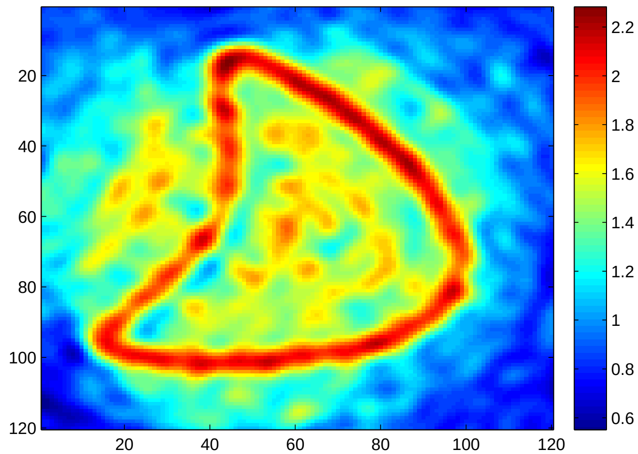

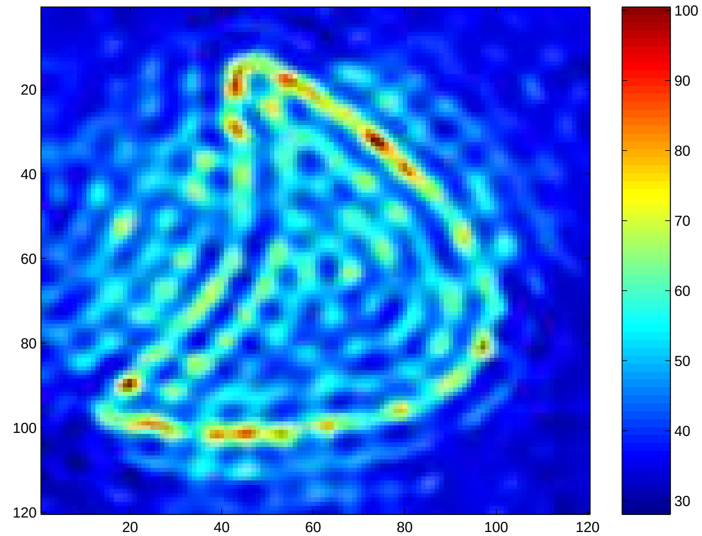

200% noise $\lambda = 16, 24, 32h$

200% noise $\lambda = 16h$

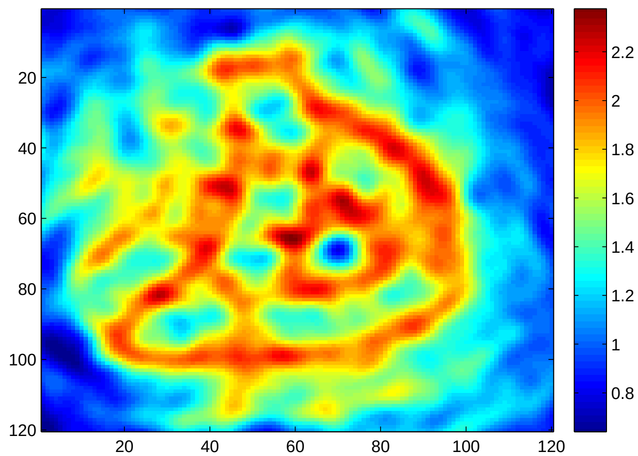

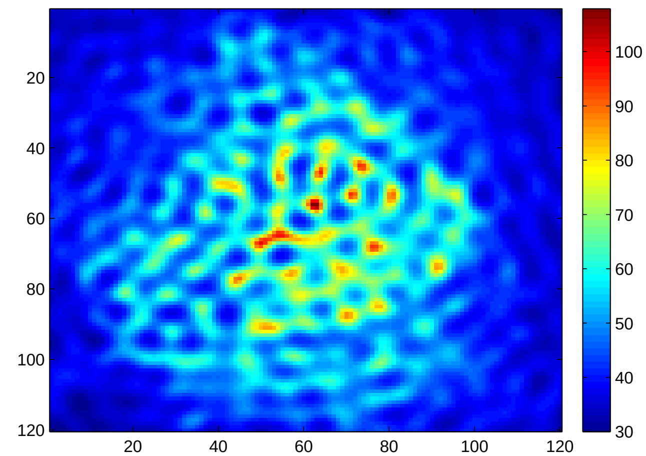

10% random medium $\lambda = 16, 24, 32h$

200% random medium $\lambda = 16h$

Future plan

- Target detection in random medium.
- Shape construction using multiple frequencies.
- Limited aperture.